SINTEF
PROCEEDINGS
2

Proceedings of the 12th International Conference on Computational Fluid Dynamics in the Oil & Gas, Metallurgical and Process Industries

Progress in Applied CFD – CFD2017

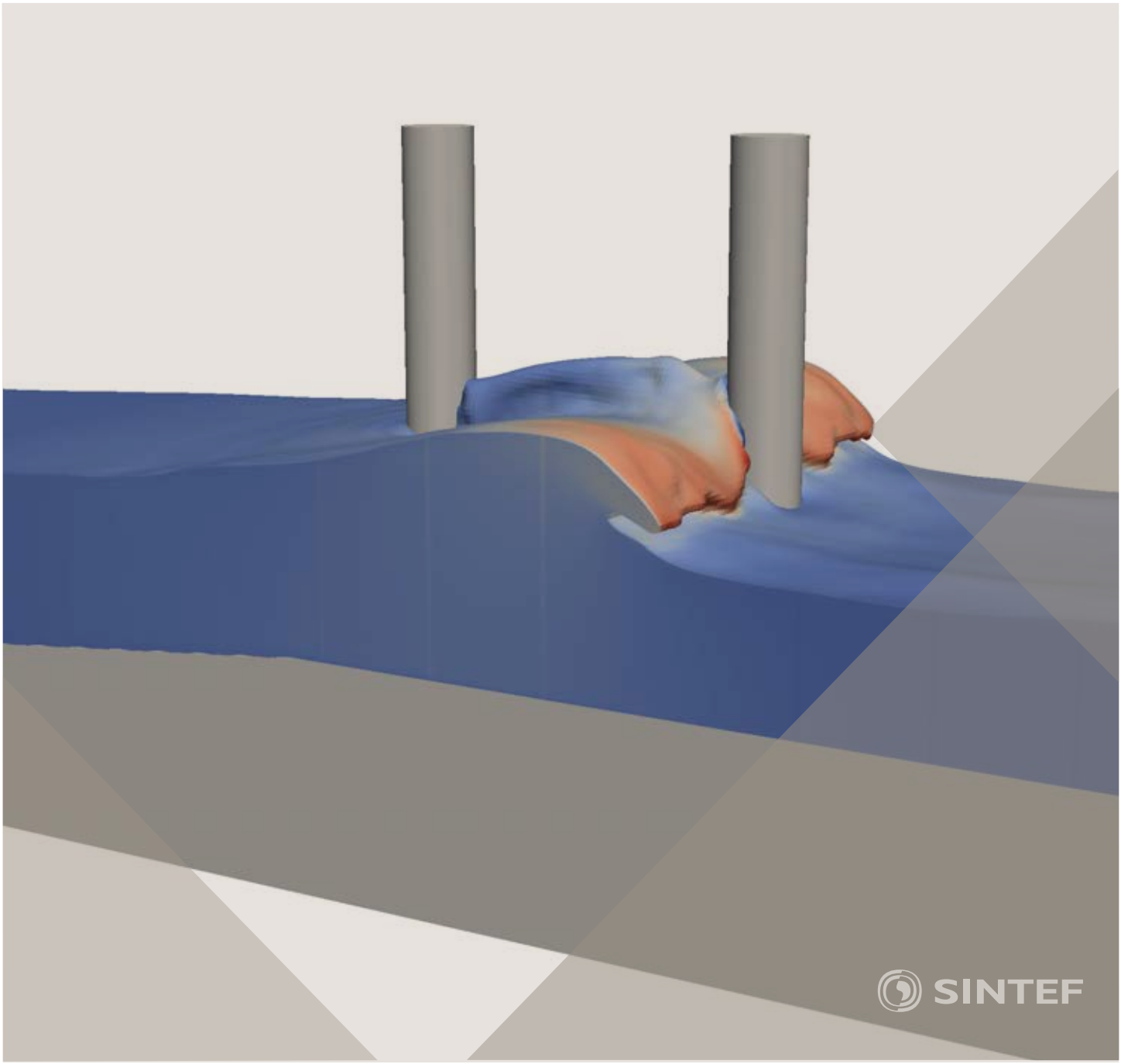

SINTEF Proceedings

Editors:
Jan Erik Olsen and Stein Tore Johansen

Progress in Applied CFD – CFD2017

Proceedings of the 12th International Conference on Computational Fluid Dynamics in the Oil & Gas, Metallurgical and Process Industries

SINTEF Academic Press

SINTEF Proceedings no 2
Editors: Jan Erik Olsen and Stein Tore Johansen
Progress in Applied CFD – CFD2017
Selected papers from 10th International Conference on Computational Fluid Dynamics in the Oil & Gas, Metallurgical and Process Industries

Key words:
CFD, Flow, Modelling

Cover, illustration: Arun Kamath

ISSN 2387-4295 (online)
ISBN 978-82-536-1544-8 (pdf)

SINTEF Academic Press
Address: Forskningsveien 3 B
PO Box 124 Blindern
N-0314 OSLO
Tel: +47 73 59 30 00
Fax: +47 22 96 55 08

www.sintef.no/byggforsk
www.sintefbok.no

SINTEF Proceedings
SINTEF Proceedings is a serial publication for peer-reviewed conference proceedings on a variety of scientific topics.
The processes of peer-reviewing of papers published in SINTEF Proceedings are administered by the conference organizers and proceedings editors. Detailed procedures will vary according to custom and practice in each scientific community.

PREFACE

This book contains all manuscripts approved by the reviewers and the organizing committee of the 12th International Conference on Computational Fluid Dynamics in the Oil & Gas, Metallurgical and Process Industries. The conference was hosted by SINTEF in Trondheim in May/June 2017 and is also known as CFD2017 for short. The conference series was initiated by CSIRO and Phil Schwarz in 1997. So far the conference has been alternating between CSIRO in Melbourne and SINTEF in Trondheim. The conferences focuses on the application of CFD in the oil and gas industries, metal production, mineral processing, power generation, chemicals and other process industries. In addition pragmatic modelling concepts and bio-mechanical applications have become an important part of the conference. The papers in this book demonstrate the current progress in applied CFD.

The conference papers undergo a review process involving two experts. Only papers accepted by the reviewers are included in the proceedings. 108 contributions were presented at the conference together with six keynote presentations. A majority of these contributions are presented by their manuscript in this collection (a few were granted to present without an accompanying manuscript).

The organizing committee would like to thank everyone who has helped with review of manuscripts, all those who helped to promote the conference and all authors who have submitted scientific contributions. We are also grateful for the support from the conference sponsors: ANSYS, SFI Metal Production and NanoSim.

Stein Tore Johansen & Jan Erik Olsen

Organizing committee:

Conference chairman: Prof. Stein Tore Johansen
Conference coordinator: Dr. Jan Erik Olsen
Dr. Bernhard Müller
Dr.Sigrid Karstad Dahl
Dr.Shahriar Amini
Dr.Ernst Meese
Dr.Josip Zoric
Dr.Jannike Solsvik
Dr.Peter Witt

Scientific committee:

Stein Tore Johansen, SINTEF/NTNU
Bernhard Müller, NTNU
Phil Schwarz, CSIRO
Akio Tomiyama, Kobe University
Hans Kuipers, Eindhoven University of Technology
Jinghai Li, Chinese Academy of Science
Markus Braun, Ansys
Simon Lo, CD-adapco
Patrick Segers, Universiteit Gent
Jiyuan Tu, RMIT
Jos Derksen, University of Aberdeen
Dmitry Eskin, Schlumberger-Doll Research
Pär Jönsson, KTH
Stefan Pirker, Johannes Kepler University
Josip Zoric, SINTEF

CONTENTS

PRAGMATIC MODELLING 9
On pragmatism in industrial modeling. Part III: Application to operational drilling 11
CFD modeling of dynamic emulsion stability 23
Modelling of interaction between turbines and terrain wakes using pragmatic approach 29

FLUIDIZED BED 37
Simulation of chemical looping combustion process in a double looping fluidized bed reactor with cu-based oxygen carriers 39
Extremely fast simulations of heat transfer in fluidized beds 47
Mass transfer phenomena in fluidized beds with horizontally immersed membranes 53
A Two-Fluid model study of hydrogen production via water gas shift in fluidized bed membrane reactors 63
Effect of lift force on dense gas-fluidized beds of non-spherical particles 71
Experimental and numerical investigation of a bubbling dense gas-solid fluidized bed 81
Direct numerical simulation of the effective drag in gas-liquid-solid systems 89
A Lagrangian-Eulerian hybrid model for the simulation of direct reduction of iron ore in fluidized beds 97
High temperature fluidization - influence of inter-particle forces on fluidization behavior 107
Verification of filtered two fluid models for reactive gas-solid flows 115

BIOMECHANICS 123
A computational framework involving CFD and data mining tools for analyzing disease in cartoid artery 125
Investigating the numerical parameter space for a stenosed patient-specific internal carotid artery model 133
Velocity profiles in a 2D model of the left ventricular outflow tract, pathological case study using PIV and CFD modeling 139
Oscillatory flow and mass transport in a coronary artery 147
Patient specific numerical simulation of flow in the human upper airways for assessing the effect of nasal surgery 153
CFD simulations of turbulent flow in the human upper airways 163

OIL & GAS APPLICATIONS 169
Estimation of flow rates and parameters in two-phase stratified and slug flow by an ensemble Kalman filter 171
Direct numerical simulation of proppant transport in a narrow channel for hydraulic fracturing application 179
Multiphase direct numerical simulations (DNS) of oil-water flows through homogeneous porous rocks 185
CFD erosion modelling of blind tees 191
Shape factors inclusion in a one-dimensional, transient two-fluid model for stratified and slug flow simulations in pipes 201
Gas-liquid two-phase flow behavior in terrain-inclined pipelines for wet natural gas transportation 207

NUMERICS, METHODS & CODE DEVELOPMENT 213
Innovative computing for industrially-relevant multiphase flows 215
Development of GPU parallel multiphase flow solver for turbulent slurry flows in cyclone 223
Immersed boundary method for the compressible Navier–Stokes equations using high order summation-by-parts difference operators 233
Direct numerical simulation of coupled heat and mass transfer in fluid-solid systems 243
A simulation concept for generic simulation of multi-material flow, using staggered Cartesian grids 253
A cartesian cut-cell method, based on formal volume averaging of mass, momentum equations 265
SOFT: a framework for semantic interoperability of scientific software 273

POPULATION BALANCE 279
Combined multifluid-population balance method for polydisperse multiphase flows 281
A multifluid-PBE model for a slurry bubble column with bubble size dependent velocity, weight fractions and temperature 285
CFD simulation of the droplet size distribution of liquid-liquid emulsions in stirred tank reactors 295
Towards a CFD model for boiling flows: validation of QMOM predictions with TOPFLOW experiments 301
Numerical simulations of turbulent liquid-liquid dispersions with quadrature-based moment methods 309
Simulation of dispersion of immiscible fluids in a turbulent couette flow 317
Simulation of gas-liquid flows in separators - a Lagrangian approach 325
CFD modelling to predict mass transfer in pulsed sieve plate extraction columns 335

BREAKUP & COALESCENCE 343
Experimental and numerical study on single droplet breakage in turbulent flow 345
Improved collision modelling for liquid metal droplets in a copper slag cleaning process 355
Modelling of bubble dynamics in slag during its hot stage engineering 365
Controlled coalescence with local front reconstruction method 373

BUBBLY FLOWS 381
Modelling of fluid dynamics, mass transfer and chemical reaction in bubbly flows 383
Stochastic DSMC model for large scale dense bubbly flows 391
On the surfacing mechanism of bubble plumes from subsea gas release 399
Bubble generated turbulence in two fluid simulation of bubbly flow 405

HEAT TRANSFER 413
CFD-simulation of boiling in a heated pipe including flow pattern transitions using a multi-field concept 415
The pear-shaped fate of an ice melting front 423
Flow dynamics studies for flexible operation of continuous casters (flow flex cc) 431
An Euler-Euler model for gas-liquid flows in a coil wound heat exchanger 441

NON-NEWTONIAN FLOWS 449
Viscoelastic flow simulations in disordered porous media 451
Tire rubber extrudate swell simulation and verification with experiments 459
Front-tracking simulations of bubbles rising in non-Newtonian fluids 469
A 2D sediment bed morphodynamics model for turbulent, non-Newtonian, particle-loaded flows 479

METALLURGICAL APPLICATIONS 491
Experimental modelling of metallurgical processes 493
State of the art: macroscopic modelling approaches for the description of multiphysics phenomena within the electroslag remelting process 499
LES-VOF simulation of turbulent interfacial flow in the continuous casting mold 507
CFD-DEM modelling of blast furnace tapping 515
Multiphase flow modelling of furnace tapholes 521
Numerical predictions of the shape and size of the raceway zone in a blast furnace 531
Modelling and measurements in the aluminium industry - Where are the obstacles? 541
Modelling of chemical reactions in metallurgical processes 549
Using CFD analysis to optimise top submerged lance furnace geometries 555
Numerical analysis of the temperature distribution in a martensic stainless steel strip during hardening 565
Validation of a rapid slag viscosity measurement by CFD 575
Solidification modeling with user defined function in ANSYS Fluent 583
Cleaning of polycyclic aromatic hydrocarbons (PAH) obtained from ferroalloys plant 587
Granular flow described by fictitious fluids: a suitable methodology for process simulations 593
A multiscale numerical approach of the dripping slag in the coke bed zone of a pilot scale Si-Mn furnace 599

INDUSTRIAL APPLICATIONS 605
Use of CFD as a design tool for a phospheric acid plant cooling pond 607
Numerical evaluation of co-firing solid recovered fuel with petroleum coke in a cement rotary kiln: Influence of fuel moisture 613
Experimental and CFD investigation of fractal distributor on a novel plate and frame ion-exchanger 621

COMBUSTION 631
CFD modeling of a commercial-size circle-draft biomass gasifier 633
Numerical study of coal particle gasification up to Reynolds numbers of 1000 641
Modelling combustion of pulverized coal and alternative carbon materials in the blast furnace raceway 647
Combustion chamber scaling for energy recovery from furnace process gas: waste to value 657

PACKED BED 665
Comparison of particle-resolved direct numerical simulation and 1D modelling of catalytic reactions in a packed bed 667
Numerical investigation of particle types influence on packed bed adsorber behaviour 675
CFD based study of dense medium drum separation processes 683
A multi-domain 1D particle-reactor model for packed bed reactor applications 689

SPECIES TRANSPORT & INTERFACES 699
Modelling and numerical simulation of surface active species transport - reaction in welding processes 701
Multiscale approach to fully resolved boundary layers using adaptive grids 709
Implementation, demonstration and validation of a user-defined wall function for direct precipitation fouling in Ansys Fluent 717

FREE SURFACE FLOW & WAVES 727
Unresolved CFD-DEM in environmental engineering: submarine slope stability and other applications 729
Influence of the upstream cylinder and wave breaking point on the breaking wave forces on the downstream cylinder 735
Recent developments for the computation of the necessary submergence of pump intakes with free surfaces 743
Parallel multiphase flow software for solving the Navier-Stokes equations 752

PARTICLE METHODS 759
A numerical approach to model aggregate restructuring in shear flow using DEM in Lattice-Boltzmann simulations 761
Adaptive coarse-graining for large-scale DEM simulations 773
Novel efficient hybrid-DEM collision integration scheme 779
Implementing the kinetic theory of granular flows into the Lagrangian dense discrete phase model 785
Importance of the different fluid forces on particle dispersion in fluid phase resonance mixers 791
Large scale modelling of bubble formation and growth in a supersaturated liquid 798

FUNDAMENTAL FLUID DYNAMICS 807
Flow past a yawed cylinder of finite length using a fictitious domain method 809
A numerical evaluation of the effect of the electro-magnetic force on bubble flow in aluminium smelting process 819
A DNS study of droplet spreading and penetration on a porous medium 825
From linear to nonlinear: Transient growth in confined magnetohydrodynamic flows 831

CFD MODELLING TO PREDICT MASS TRANSFER IN PULSED SIEVE PLATE EXTRACTION COLUMNS

Nirvik SEN[1*], K.K. SINGH[1,2], A.W. PATWARDHAN[3], S. MUKHOPADHYAY[1,2], K.T SHENOY[2], S. MOHAN[4]
[1]Homi Bhabha National Institute, Mumbai, INDIA
[2]Chemical Engineering Division, Bhabha Atomic Research Centre, Mumbai, INDIA
[3]Institute of Chemical Technology, Mumbai, INDIA
[4]Chemical Engineering Group, Bhabha Atomic Research Centre, Mumbai, INDIA
Corresponding author's e-mail: nirvik@barc.gov.in

ABSTRACT

A 2D CFD-PBM based numerical model to predict interphase mass transfer in a Pulsed Sieve Plate Column (PSPC) is reported. The model is based on Euler-Euler interpenetrating continuum approach. Drag law due to Schiller and Naumann is used to model the interphase momentum exchange term. Spatial and temporal variations of drop population are obtained by coupling Population Balance (PB) equations with flow equations. Suitable drop coalescence and breakage kernels are used in the PB equations. Species transport equation is solved in both phases to predict interphase mass. The developed model is validated against reported mass transfer experimental data in a 2 inch PSPC. Absolute average error in prediction is less than 5%. The validated model is used to understand the complex time periodic flow patterns inside the column.

Keywords: CFD, population balance equations, two phase flow, species transport equations, mass transfer. snap-shot approach.

NOMENCLATURE

Greek Symbols

β Coalescence kernel
ϕ Phase fraction, [-].
λ Collision efficiency, [-].

Latin Symbols

A Pulse amplitude, [m].
a Breakage kernel,
B^a Droplet birth due to aggregation, [1/m^3-s].
B^b Droplet birth due to breakage, [1/m^3-s].
b Daughter droplet distribution
D^a Droplet death due to aggregation, [1/m^3-s].
D^b Droplet death due to aggregation, [1/m^3-s].
D Effective diffusion coefficient, [m2/s].
f Pulse frequency, [1/s].
h Collision frequency [1/m^3-s]
K_d Distribution coefficient, [-].
K_La Overall volumetric mass transfer coefficient, [1/s].
L Characteristic drop size, [m].
n Droplet number density, [m/s].
$\boldsymbol{U}$ Velocity vector, [m/s].
U_p Pulsing velocity, [m/s]
x Concentration of solute in aqueous phase, [-].
y Concentration of solute in organic phase, [-].

Subscripts

p p^{th} *phase.*
q q^{th} *phase.*
j j^{th} *species.*

INTRODUCTION

Pulsed sieve plate columns (PSPCs) are extensively used for solvent extraction in hydrometallurgical processes for extraction of important metal values (Grodfrey and Slator, 1994; Ferreira et al., 2010; Gameiro et al., 2010).

Typically pulsed column involves a cylindrical section comprising of plates with sieve holes. The construction is similar to that of a sieve plate. However, the percentage opening and hole size in the sieve plates are not sufficient to allow a counter-current flow (heavier aqueous phase moving downward while lighter organic phase moving upwards) solely due to gravity. Thus in a pulsed sieve plate the column contents are pneumatically pulsed from the bottom which forces the phases through the sieve plates ensuring counter-current flow in the column. During the positive peak of the pulse the lighter phase is forced up through the sieve holes. In doing so the lighter phase breaks up into small drops which increase the specific interfacial area for mass transfer. Pulsing also increases the turbulence in the column which increases the mass transfer coefficients. Thus a PSPC becomes more efficient than a typical sieve plate column.

PSPCs are characterised by high mass transfer efficiency and higher throughput. Another feature of PSPC is absence of any moving part which makes these columns highly reliable and maintenance-free. Even though there has been a large volume of work on PSPCs, most of it is experimental. There have been experimental studies on pressure drop and axial dispersion in two-phase flow (Miyauchi and Oya, 1965; Novotny et al., 1970; Rao et al., 1978; Srinikethan et al., 1987). Experimental studies on mass transfer, dispersed phase hold up and drop size distribution have also been reported (Kumar and Hartland, 1988; Lorenz et al., 1990; Srinivasulu et al., 1997; Kumar and Hartland, 1999; Usman et al., 2009). Several experimental studies shed light on different regimes of operation and transitions from one regime to another (Sato et al., 1963; Boyadzhiev and Spassov, 1982; Kumar and

Hartland, 1983). Experiments to understand flooding characteristics have also been reported (Kagan et al., 1965, Tronton, 1957). The end results of most of the experimental studies on PSPCs are empirical correlations. Due to the large volume of experimental work that has been carried out, there exist many empirical correlations for PSPCs. Each of these correlations is valid for the range of the experimental data over which it has been regressed. However, there is no correlation that has been shown to be universal enough to be valid over a wide range of operational and design parameters. The existence of so many correlations has in fact caused a "problem of plenty" making it difficult to choose the best correlations to be used for designing a PSPC for a given duty (Yadav and Patwardhan, 2008).

As a result, design of industrial scale PSPCs still is based on the data generated using pilot-scale units and insights into the local hydrodynamics in the column are still rare. It becomes very difficult to experimentally investigate local hydrodynamics and drop dynamics in a column, especially large diameter columns. This makes use of CFD-based models very attractive. Such models can provide valuable insights into the functioning of the columns, help reduce experimentation and design of industrial-scale columns.

CFD and CFD coupled with population balance modleing (PBM) have been used to model dispersed liquid-liquid two-phase flow in different types of equipments (Wang and Mao, 2005; Gimbun et al., 2009; Kerdouss et al., 2008). Recently, several studies on CFD modelling of air pulsed columns have also been reported. But majority of these studies are on pulsed disc and doughnut columns (Retieb el al., 2007; Nabli et al., 1997; Saini and Bose, 2014). A CFD-PBM based approach to model pulsed disc and doughnut column was reported by Amokrane and coworker (Amokrane et al., 2014). Only drop breakage was considered in PBM. Single-phase CFD model was validated using experimental PIV data. The PBM was validated separately using the experimental data generated in a stirred tank. There after coupled CFD-PBM was used to predict the hydrodynamics in the column. However, the results of the CFD-PBM based model were not validated. In a recent study by the same group (Amokrane et al., 2016) a CFD-PBM approach considering both drop breakage and coalescence was reported. Drop size distribution in a 1 inch column was measured and used for optimization of the breakage and coalescence kernels. Only limited validation of the CFD-PBM approach was reported. Though there are several single-phase CFD studies on PSPCs (Kolhe et al., 2011; Xiaojin and Guangsheng, 2011; Sen et al., 2015) two-phase CFD studies on PSPCs are scarce. Yadav and Patwardhan, 2009 reported two-phase CFD modeling of a PSPC to study the effects of pulsing on column hydrodynamics, operating regimes and dispersed phase hold-up. However, the plates used in their work had downcomer (separate path/passage provided for the heavier phase to move down the column – similar to those provided in sieve/bubble cap plates in distillation columns for the downward movement of the heavier liquid phase). Plates typically used in PSPCs do not have downcomers. The hydrodyanmics in a column having plates with downcomers may be significantly different from those without downcomer. Din et al., 2010 reported a 2D two-phase CFD model of PSPC but the sieve plate section was modelled as a porous medium which is a significant simplification of the actual geometry. Recently we reported a 2D two-phase CFD mdoel to predict hydrodynamics and dispersed phase holdup in PSPC (Sen et al., 2016). A comparison of different drag models, was carried out and validation against reported experimental data was done. To the best of our knowledge CFD-PBM simulation of PSPCs has not been reproted so far. This study, therefore, represents the first implementation of CFD-PBM approach for PSPCs.

1D mathematical models to predict mass transfer in PSPCs have also been reported (Gonda and Matsuda, 1986; Torab-Mostaedi and Safdari, 2009). In fact, in nuclear fuel cycle several codes based on 1 D modelling are available (SOLVEX, SEPHIS-MOD4, Revised MIXSET, PULCO). However, each of these mathematical models embed several empirical correlations. With each correlation having its own uncertainty, using several of them in a mathematical model may result in significant overall uncertainty in the predictions of the model.

In the present work, we report, for the first time, 2D two-phase CFD-PBM simulations to directly predict mass transfer of a species/solute from organic to aqueous phase in a PSPC. The model is developed and validated against reported experimental data of a 2 inch diameter PSPC. The model provides insights into spatial and temporal variations of hydrodynamic variables inside the column under pulsing conditions and resultant effect on mass transfer in a 2D computational domain.

MODEL DESCRIPTION

Computational approach

Two fluid Euler–Euler approach was used to model two phase liquid-liquid flow in PSPC using a commerical finite volume based code. This approach has been widely used to simulate dispersed two-phase flows (Yadav and Patwardhan, 2009; Din et al., 2010; Ranade, 2002; Wang et al., 2014). The model solves the conservation equations for momentum and mass for both phases and assumes that both the phases can co-exist in every computational cell in the domain. The phase fraction (or hold up) of the dispersed phase in each cell is computed by solving a convection-diffusion transport equation for the phase fraction itself. The momentum exchange between the two phases is modelled through the interphase exchange coefficients which in turn is defined in terms of a drag coefficient.

Turbulence has been modelled using the mixture k-ε model in which the turbulence equations are solved for the mixture as a whole. This approach reduces the number of equations to be solved thus reducing computational time. The relevent equations can be found elsewhere (Sen et al., 2016) and are ommited here for brevity.

The exchange of momentum between the phases is only through the drag force which is quantified using the drag model of Schiller and Naumann.

One major simplification in two-phase CFD simulations of PSPCs reported till now has been the assumption of monodispersed drops. In such models the information on temporal and spatial variations of drop size is lost. In the present work a predictive CFD-PBM numerical approach is used to circumvent the monodispersed approximation in computational models of PSPCs. The method of classes is used to solve the population balance model (PBM).

Local drop size distribution inside PSPC depends on the initial drop size distribution in the feed, convective transport of the drops, breakage and coalescence rates of drops. In absence of mass transfer, the population balance equation for characteristic length of drop (L) can be written as (Singh et al., 2009; Marchisio et al., 2003)

$$\frac{\partial}{\partial t}\{n(L,t)\} + \nabla.(\boldsymbol{U}.n(L,t)) = B^a(L;t) - D^a(L;t) + B^b(L;t) - D^b(L;t) \quad (1)$$

Here B^a and B^b are birth rates of droplet of size L at any time t due to coalescence and breakage respectively. $D^a$and $D^b$are the death rates of droplet of size L at any time t due to coalescence and breakage, respectively. $n(L;t)$ is number density (per unit volume) of droplet having characteristic length L at any time t.

The expressions for the birth and death rates are given by Eq. (2) to (5).

$$B^a(L;t) = \frac{L^2}{2}\int_0^L \frac{\beta\{(L^3-\lambda^3)^{1/3},\lambda\}}{(L^3-\lambda^3)^{2/3}} n\{(L^3-\lambda^3)^{1/3};t\}n(\lambda;t)d\lambda \quad (2)$$

$$D^a(L;t) = n(L;t)\int_0^\infty \beta(L,\lambda)n(\lambda;t)d\lambda \quad (3)$$

$$B^b(L;t) = \int_L^\infty a(\lambda)b(L|\lambda)n(\lambda;t)d\lambda \quad (4)$$

$$D^b(L;t) = a(L)n(L;t) \quad (5)$$

Where, β is the coalescence kernel, a is the breakage kernel, b is the daughter droplet distribution, $h(L,\lambda)$ and $\eta(L,\lambda)$ are collision frequency and collision efficiency, respectively. In literature, several kernels have been reported.

Breakage, daughter droplet distribution and coalescence kernels (and constants there in) proposed by Hsia and Tavlarides (Hsia and Tavlarides, 1980) have been used in the present work. Expression for these kernels are available elsewhere (Hsia and Tavlarides, 1980; Singh et al., 2009) and are omitted here for brevity.

The entire range of possible droplet size is divided into a fixed number of classes and a conservation euqation is solved for each class. The rate of death and birth of drops in a specific class due to breakage and coalescense are accounted using respective kernels. In the presnt work, the range of drop sizes is considered to be from 0.5 mm to 4 mm. This choice of drop size is based on the values of drop sizes typically observed in a pulsed column (Lorentz et al., 1990, Usman et al., 2006).

Mass transfer of j^{th} solute (concentration x_j) from one phase (phase p) to the other phase (phase q) is modelled by solving species transport equation in both phases with mass exchange (source) terms as shown in Eqn. (6-7). Concentration of solute in the second phase (phase q) is denoted by y_j.

$$\frac{\partial x_j}{\partial t}\phi_P + \phi_P \boldsymbol{U}.\nabla x_j = \phi_P D_P \nabla^2 x_j - K_L a\left(x_j - \frac{y_j}{K_d}\right) \quad (6)$$

$$\frac{\partial y_j}{\partial t}\phi_q + \phi_q \boldsymbol{U}.\nabla y_j = \phi_q D_q \nabla^2 y_j + K_L a\left(x_j - \frac{y_j}{K_d}\right) \quad (7)$$

where ϕ_p is hold up of the p^{th} phase, D is the effective diffusivity (comprising of both eddy and molecular diffusion), K_La is overall volumetric mass transfer coefficient, K_d is the distribution coefficient. Value of K_La and K_d are estimated from the correlations reported in literature (Gonda and Matsuda, 1986). The mass transfer term (source term) is calculated based on the difference in concentration of the solute in the two phases and overall volumetric mass transfer coefficient. The two species transport equations are coupled with each other through the source terms. As the problem involves partitioning of one solute in two different phases, solute concentrations in the organic and the aqueous phases are related through the following equation.

$$y_j = K_d x_j \quad (8)$$

The pulsing action is introduced into the computational model using a pusatile velocity at the pulse inlet, as given by Eq. (9).

$$U_P = \pi A f\, Sin(2\pi f t) \quad (9)$$

where U_p is the pulsing velocity, A is the amplitude and f is frequency (Hz) of pulsation.

As the solute concentration varies across the computational domain the density of both phases also varies. In other words as the solute is partitioned from organic phase into aqueous phase, the density of the organic phase reduces while that of the continuous phase increases. This effect has been incorporated in the model.

Computational domain

For validation of the developed model, reported experimental data on solute end concentrations in a 2 inch PSPC are used (Gonda and Matsuda, 1986). Hence, the computational domain is based on the reported geometry. A standard sieve plate cartridge (23% opening area, 3 mm hole diameter, 5 cm inter-plate spacing) was used. The column was 2 m in height and had 36 plates. A pulse leg was connected the bottom disengagement section to provide pulsation to the column contents. The phase system used was 30% TBP in dodecane and 0.1 N Nitric acid.

In the present 2D computational model a reduced number of plates (5 plates) has been considered so as to limit the size of the computational domain and the resulting computational time. Suitability of using a 2D model and reduced number of plates for CFD modelling of PSPCs has been reported earlier (Kolhe et al., 2011; Yadav and Patwardhan, 2009; Sen et al., 2015; Sen et al., 2016). Transient simulations are carried out with a

time step of 0.01 sec which corresponds to Courant numbers less than 0.5 in all cases. A grid density of 1.027 x 10^6 cells/m^2 has been used in the present work. This grid density is chosen based on the results of grid independece test carried out in our previous study on single-phase flow in pulsed sieve plate column (Sen et al., 2015). Similar grid density has been used in our recent work on two-phase flow in PSPC (Sen et al., 2016). In the model the hole diameter is kept at the original value (i.e. 3 mm) while the pitch is chosen such that percent free area is the same as in experimental setup. Fig. 1 shows the meshed computational domain and the quality of mesh in two inter-plate zones.

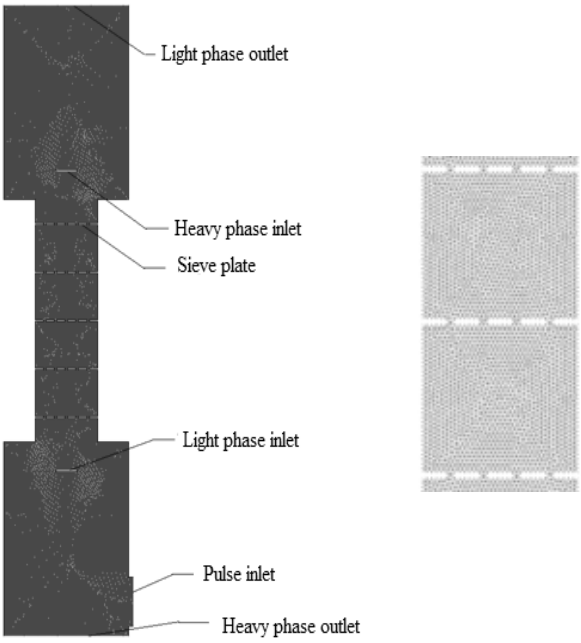

Figure 1: Meshed computational domain used to model 2 inch PSPC and zoomed view of the mesh in two inter-plate zones

RESULTS AND DISCUSSION

Validation

The mass transfer prediction of the developed CFD-PBM model is first validated against reported experimental results. Gonda and co-workers (Gonda and Matsuda, 1986) reported back extraction (stripping) of heavy metal solute from organic (dispersed phase) to aqueous (continuous phase) in a 2 inch diameter PSPC. Solute concentration in the organic phase fed to the column bottom was 97 gpl while the aqueous phase did not contain any solute. Solute concentration in each phase was reported at various locations along the column height leading to a solute concentration profile of each phase.

The computational model used in this work comprises of only 5 plates to ensure that computational time remains with in resonable limits. Solute concentration in organic phase entering the column and solute concetration in aqueous phase at the location of 5th plate from bottom goes into the model as inputs while the model predicts solute concentration in the aqueous phase exiting 1st plate from column bottom and in the organic phase exiting 5th plate from column bottom. Table 1 below shows the comparison of the predicted and reported values of solute concentration in the organic phase at the 5th plate from bottom and in the aqueous phase at the location of 1st plate from column bottom. It is seen that the absolute average error in prediction of our model is 2.8 %. Hence the 2D CFD-PBM approach can directly predict mass transfer from one phase to another with good accuracy.

Table 1: Comparison of CFD_PBM predicted values against experimental data

	CFD (gpl)	Experimental (gpl)	Average Error (%)
Solute concentration at 5th plate (from bottom) in organic phase	87.21	91.38	2.78
Solute concentration at 1st plate (from bottom) in aqueous phase	48.504	49	

Local hydrodynamic and mass transfer aspects

In this section we use the validated numerical model to understand the complex hydrodynamics in PSPC and its resultant effect on transport of species from one phase to another. Fig. 2 shows the spatial variations of dispersed phase hold up and Sauter mean drop diameter in a typical inter-plate zone. As the flow field is time varying due to pulsation the spatial variations are shown at positive peak of the pulse.

Accumulation of the dispersed phase is clearly seen below the sieve plates. The spatial variation of Sauter mean drop diameter reveals that drop of smaller size are formed at the location of the sieve holes and drop diameter increases as the dispersion moves above. This is due to the fact that turbulence dissipation rates are higher at the location of the holes (as evident from Fig. 3) which leads to increased breakage rates causing smaller drops at sieve holes. As the dispersion moves up and reaches the next plate drops tend to coalesce and increase in size. Fig. 3 shows the spatial variations of the turbulence dissipation rates, axial velocity of the continuous phase and axial velocity of the dispersed phase at the positive peak of the pulsing cycle.

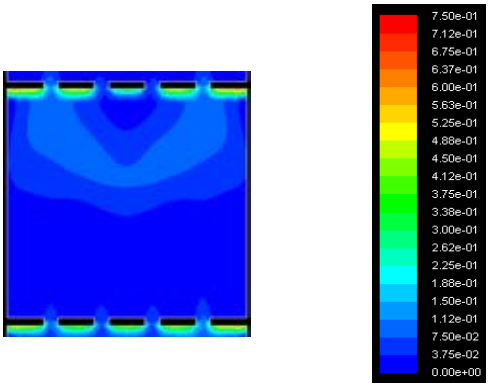

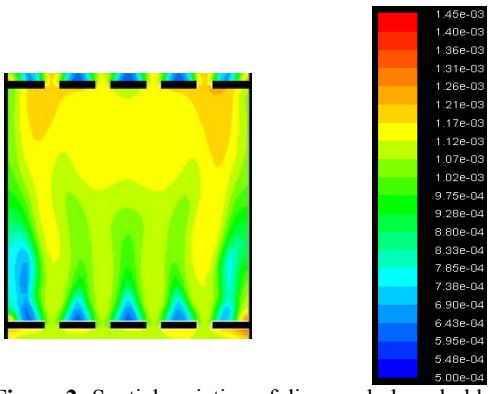

Figure 2: Spatial variation of dispersed phase hold up (-) (top) and Sauter mean drop diameter (m) (bottom)

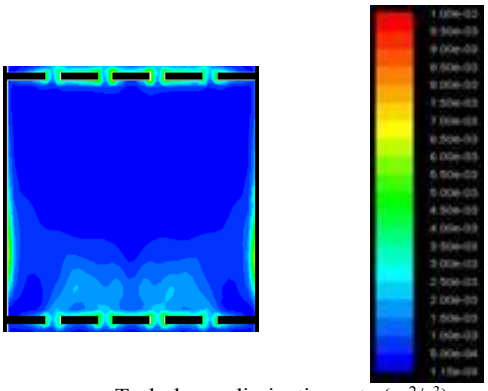

Turbulence dissipation rate (m^2/s^3)

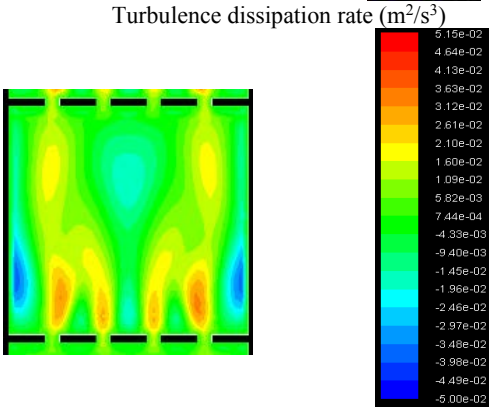

Axial velocity of the continuous phase (m/sec)

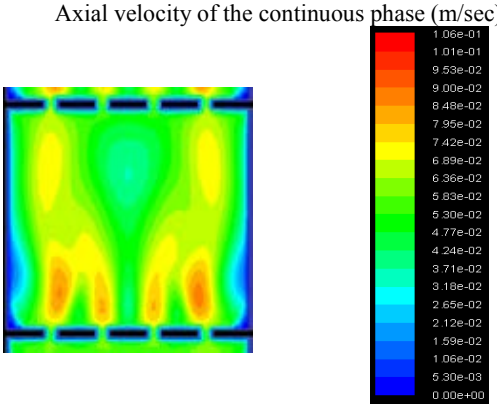

Axial velocity of the dispersed phase (m/sec)

Figure 3: Spatial variations of turbulence dissipation rate, axial velocity of continuous phase, and axial velocity of the dispersed phase

It is seen that during the up stroke (i.e. positive peak of the pulse) both phases are being pushed up through the holes (indicated by positive axial velocities at the holes even though the general direction of flow of the continuous phase is downwards. Presence of small re-circulations in the continuous phase visible near the wall (as evidenced by negative values of axial velocity of the continuous phase the wall). However, no circulations are observed for the dispersed phase as axial velocities are positive everywhere.

Fig. 4 shows the solute concentration (in terms of solute mass fraction) in the organic (dispersed) phase and the aqueous (continuous) phase.

A gradual decrease in concentration of the solute as the dispersed phase moves up is clearly observed. At the same time whatever solute leaves the dispersed (organic) phase is transferred to the continuous (aqueous) phase and is reflected as an increase in the solute concentration in the continuous phase as it flows downward.

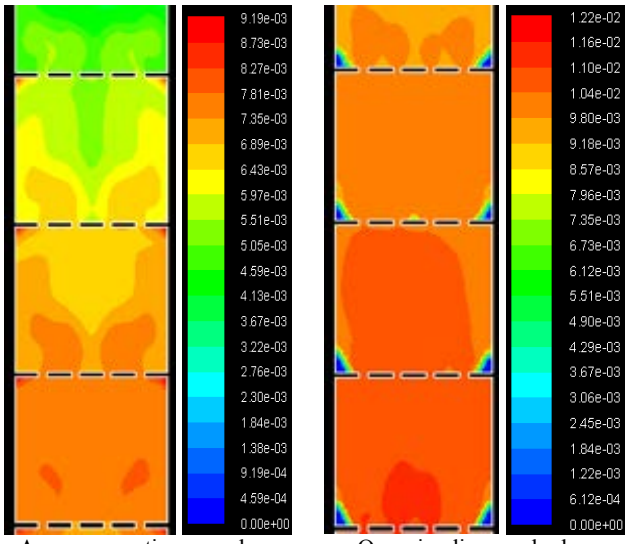

Aqueous continuous phase Organic dispersed phase

Figure 4: Spatial variations of solute mass fraction in continuous and dispersed phase.

Fig. 5 shows the spatial variation of the density of the organic phase in the entire computational domain. It is seen that density of the dispersed phase decreases as it flows upward along the column. In the model densities of both phases are composition dependent. Thus the density of the dispersed phase (organic) is seen to reduce as solute is transferred from the organic phase to the aqueous phase.

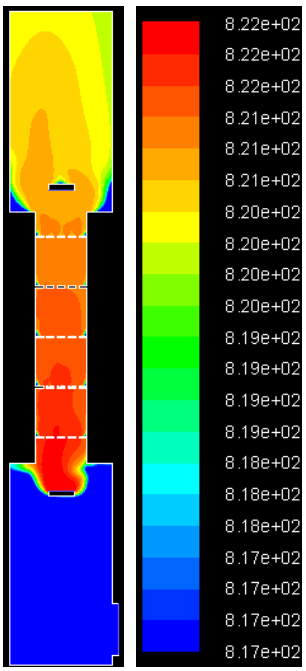

Figure 5: Spatial variation of the density of the dispersed phase (kg/m^3)

CONCLUSION

The following conclusions could be drawn from this work

1) A 2D CFD-PBM numerical model is developed which could predict spatial and temporal variations of two-phase hydrodynamics and resultant inter-phase mass transfer in a pulsed sieve plate extraction column (PSPC).

2) The model is validated against reported experimental data on solute concentration in organic and aqueous phases in a 2 inch PSPC. The model predictions are very close to reported values, the absolute average error being 2.78%.

3) The validated model is then used to understand the spatial variations of different hydrodynamics parameters like dispersed phase hold up, Sauter mean drop diameter, turbulence dissipation rate and continuous and dispersed phase axial velocities. Transfer of mass from organic phase to aqueous was also clearly captured along the computational domain.

4) The model provides a way to directly estimate mass transfer performance of a PSPC from first principles with minimum empirical inputs.

REFERENCES

AMOKRANE, A., CHARTON, S., LAMADIE, F., PAISANT, J. F. and PUEL, F., (2014), "Single-phase flow in a pulsed column: Particle Image Velocimetry Validation of a CFD based model", *Chemical Engineering Science*, **114**, 40-50.

AMOKRANE, A., MAAß, S., LAMADIE, F., PUEL, F. and CHARTON, S., (2016), "On droplets size distribution in a pulsed column. Part I: In-situ measurements and corresponding CFD–PBE simulations", *Chemical Engineering Journal*, **296**, 366-376.

BOYADZHIEV, L. and SPASSOV, M., (1982), "On the size of drops in pulsed and vibrating plate extraction columns", *Chem. Eng. Sci.*, 37: 337–340.

DIN, G.U., CHUGHTAI, I.R., INAYAT, M.H. and KHAN, I.H., (2010), "Modeling of a two-phase countercurrent pulsed sieve plate extraction column - A hybrid CFD and radiotracer RTD analysis approach", *Separation and Purification Technology*, **73 (2)**, 302-309.

FERREIRA, A.E., AGARWAL, S., MACHADO, R., GAMEIRO, M.L.F., SANTOS, M., REIS, T.A., ISMAEL, M.R.C., CORREIA, J.N., CARVATHO, J.M.R., (2010), "Extraction of copper from acidic leach solution with Acorga M5640 using a pulsed sieve plate column". *Hydrometallurgy*, **104(1)**, 66-75.

GAMEIRO**,** M.L.F., MACHADO**,** R.M., ISMAEL**,** M.R.C., REIS, T.A., CARVATHO, J.M.R.,(2010),"Copper extraction from ammoniacal medium in a pulsed sieve-plate column with LIX 84-I", *J. Hazardous Materials*, **183 (1-3)**, 165-175.

GIMBUN, J., CHRIS D.R. and ZOLTAN K. N., (2009), "Modelling of mass transfer in gas–liquid stirred tanks agitated by Rushton turbine and CD-6 impeller: a scale-up study", *Chemical Engineering Research and Design,* **87(4),** 437-451.

GODFREY, J.C. and SLATER, M.J. (1994) "Liquid-Liquid Extraction Equipment", Wiley, Chichester, U.K.

GONDA, K. and MATSUDA, T., (1986), "Solvent extraction calculation model for PUREX process in pulsed sieve plate column", *J. Nuc. Sci. Tech.*, **23(10)**, 883-895.

HSIA, M. A. and TAVLARIDES, L. L., (1980), "A simulation model for homogeneous dispersion in stirred tank", *Chem. Eng. J.,* **20**, 225–236.

KAGAN, S., AEROV, M., LONIK, V. and VOLKOVA, T., (1965), "Some hydrodynamic and mass transfer problems in pulsed sieve-plate extractors", *Int. Chem. Eng.*, **5 (4)**, 656–661.

KERDOUSS, F., BANNARI, A., PROULX, P., BANNARI, R., SKRGA, M. and LABRECQUE, Y., (2008), "Two-phase mass transfer coefficient prediction in stirred vessel with a CFD model", *Computers & Chemical Engineering*, **32(8)**, 1943-1955.

KOLHE, N.S., MIRAGE, Y.H., PATWARDHAN, A.V., RATHOD, V.K., PANDEY, N.K., MUDALI, U.K. and NATARAJAN, R., (2011), "CFD and experimental studies of single phase axial dispersion coefficient in pulsed sieve plate", *Chemical Engineering Research and Design*, ***89*(10)**, 1909-1918.

KUMAR, A. and HARTLAND, S., (1983), "Correlations for dispersed phase hold-up in pulsed sieve-plate liquid–liquid extraction columns", *Chem. Eng. Res. Des.*, **61**, 248–252.

KUMAR, A., andHARTLAND, S., (1988),"Prediction of dispersed phase hold-up in pulsed perforated-plate extraction columns",*Chem. Eng. Process. Proc. Int.*, **23(1)**, 41–59.

KUMAR, A. andHARTLAND, S., (1999),"Correlations for prediction of mass transfer coefficients in single

drop systems and liquid–liquid extraction columns",*Chem. Eng. Res. Des.*, **77 (5)**, 372–384.

LORENZ, M.,HAVERLAND, H., andVOGELPOHL, A., (1990),"Fluid dynamics of pulsed sieve plate extraction columns",*Chem. Eng. Technol.,***13(1)**, 411–422.

MARCHISIO, D. L., VIGIL, R. D. and FOX, R. O., (2003), "Implementation of the quadrature method of moments in CFD codes for aggregation–breakage problems", *Chemical Engineering Science*, **58(15)**, 3337-3351.

MIYAUCHI, T. and OYA, H., (1965),"Longitudinal dispersion in pulsed perforated-plate columns", *AIChEJ*, **11(3),** 395 402.

NABLI, M.S.A., GUIRAUD, P. and GOURDON, C., (1997), "Numerical experiment: a tool to calculate axial dispersion coefficient in disc and doughnut pulsed extraction column", *Chem. Eng. Sci.*, **52 (14)**, 2353–2368.

NOVOTNY, P.,PROCHAZKA, J., andLANDAU, J., (1970),"Axial dispersion study of single phase",*Can. J. Chem. Eng.*, **48 (8)**, 405–410.

RAO, K.V.K.,JEELANI, S.A.K., andBALSUBRAMANIAN, G.R., (1978),"Backmixing in pulsed perforated plate columns",*Can. J. Chem. Eng.*, **56(1)**, 120 - 123.

RETIEB, S., GUIRAUD, P., ANGELOV, G. and GOURDON, C., (2007), "Hold-up within two-phase counter current pulsed columns via Eulerian simulations", *Chem. Eng. Sci.*, **62(17)**, 4558-72.

SAINI, R.K. and BOSE, M., (2014), "Stage holdup of dispersed phase in disc & doughnut pulsed column", *Energy Procedia*, **54**, 796-803.

SATO, T., SUGIHARA, K., and TANIYAMA, I., (1963), "Performance characteristics of pulsed perforated plate columns", *Kogaku Kogaku*, **27,** 583–586.

SEN, N., SINGH, K.K., PATWARDHAN, A.W., MUKHOPADHYAY, S. and SHENOY, K.T., (2015), "CFD Simulations of Pulsed Sieve Plate Column: Axial Dispersion in Single-Phase Flow", *Separation Science and Technology*, **50(16)**, 2485-2495.

SEN, N., SINGH, K.K., PATWARDHAN, A.W., MUKHOPADHYAY, S. and SHENOY, K.T., (2016), "CFD Simulations of two phase flow in pulsed columns: Identification of drag law", *Separation Science and Technology*, **51(17)**, 2790-2803.

SINGH, K. K., MAHAJANI, S. M., SHENOY, K. T. and GHOSH, S. K., (2009), "Population balance modelling of liquid−liquid dispersions in homogeneous continuous-flow stirred tank. *Industrial & Engineering Chemistry Research*, **48(17)**, 8121-8133.

SRINIKETHAN, G.,PRABHAKAR, A., andVARMA, Y.G.B., (1987),"Axial dispersion in plate-pulsed columns",*Bioprocess Eng.*, **2(4)**, 161-168.

SRINIVASULU, K.,VENKATNARSAIAH, D. andVARMA, Y.B.G., (1997),"Drop size distribution in liquid pulsed columns", *Bioprocess Eng.*, **17 (3)**, 189–195.

TORAB-MOSTAEDI, M. and SAFDARI, J., (2009), "Prediction of mass transfer coefficients in a pulsed packed extraction column using effective diffusivity", *Braz. J. Chem. Eng.*, **26(4)**, 685-694.

USMAN, M.R., SATTAR, H., HUSSAIN, S.N., MUHAMMAD, H., ASGHAR, A. and AFZAL, W., (2009), "Drop size in a liquid pulsed sieve plate extraction column". *Braz. J. Chem. Engg.*, **26(4)**, 677-683.

WANG, F. and MAO, Z. S., (2005), "Numerical and experimental investigation of liquid-liquid two-phase flow in stirred tanks", *Industrial & engineering chemistry research*, **44(15)**, 5776-5787.

XIAOJIN, T. and GUANGSHENG, L., (2011), "CFD simulations to flow characteristics in pulsed sieve plate extraction columns", *Ind. Eng. Chem. Res.*, **50 (2)**: 1110-1114.

YADAV, R.L. and PATWARDHAN, A.W., (2008), "Design aspects of pulsed sieve plate columns", *Chem. Eng. J.*, **138(1-3)**, 389-415.

YADAV, R.L. and PATWARDHAN, A.W., (2009), "CFD modeling of sieve and pulsed- sieve plate extraction columns", *Chem. Eng. Res. Des.*, **87 (1)**, 25–35.